RESEARCH MEMORANDUM

EXPERIMENTAL INVESTIGATION OF THE TRANSONIC AND

SUPERSONIC FLUTTER CHARACTERISTICS OF THE

UPPER AND LOWER VERTICAL TAILS OF

AN AIR-TO-GROUND MISSILE

By Perry W. Hanson and A. Gerald Rainey

Langley Aeronautical Laboratory
Langley Field, Va.

NATIONAL ADVISORY COMMITTEE
FOR AERONAUTICS
WASHINGTON
June 5, 1957
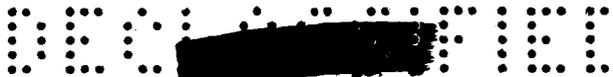
NATIONAL ADVISORY COMMITTEE FOR AERONAUTICS

RESEARCH MEMORANDUM

EXPERIMENTAL INVESTIGATION OF THE TRANSONIC AND

SUPERSONIC FLUTTER CHARACTERISTICS OF THE

UPPER AND LOWER VERTICAL TAILS OF

AN AIR-TO-GROUND MISSILE

By Perry W. Hanson and A. Gerald Rainey

SUMMARY

Flutter models of the upper and lower vertical tails of an air-to-ground missile have been tested in the Mach number range from 0.5 to 3.0. It was found that the upper surface exhibited more or less conventional flutter behavior throughout the Mach number range, whereas the lower surface experienced a sudden change in flutter mode at a Mach number of about 1.18. This change in flutter mode was accompanied by a decrease of about 50 percent in the density required for flutter to occur.

INTRODUCTION

The increased usage of highly swept surfaces for stability and control of airplanes and missiles coupled with the frequent occurrence of flutter of these surfaces has led to considerable interest in a study of their flutter characteristics. At the present time, analytical predictions of the flutter behavior of such surfaces are subject to question, particularly in the transonic speed range. Furthermore, no systematic experimental trend studies have been made so that the designer, at present, is faced with the problem of having to determine experimentally the flutter characteristics of each particular configuration he may wish to use. It is for this reason that it was considered desirable to test models of the upper and lower vertical tails of a proposed air-to-ground missile. The models were tested at Mach numbers of about 0.5 to 1.24 in the Langley 2-foot transonic flutter tunnel and at Mach numbers of 1.3 to 3.0 in the Langley 9- by 18-inch supersonic flutter tunnel.

The purpose of this paper is to present the experimentally determined flutter characteristics of these two configurations and to present the available structural information describing the models.

SYMBOLS

a   speed of sound, ft/sec

b   semichord at three-quarter-span station, ft

M   Mach number

μ mass-ratio parameter (see pages 4 and 5)

ρ density of test medium, slugs/cu ft

ω_f/ω_β ratio of flutter frequency to coupled rudder rotation frequency

APPARATUS AND TESTS

Description of Wind Tunnels

The tests were conducted in the Langley 2-foot transonic flutter tunnel for the Mach number range from 0.5 to 1.24 and in the Langley 9-by 18-inch supersonic flutter tunnel for the Mach number range from 1.3 to 3.0.

The Langley 2-foot transonic flutter tunnel is a conventional slotted-throat single-return wind tunnel equipped to use either air or Freon-12 as a test medium. This tunnel is of the continuous-operation type; that is, it is powered by a motor-driven fan. Both test section Mach number and density are continuously controllable.

The 9- by 18-inch supersonic flutter tunnel is a conventional fixed-nozzle blowdown-type wind tunnel exhausting into a vacuum sphere. The nozzle configurations used in this investigation gave Mach numbers of 1.3, 1.64, 2.0, and 3.0. At each Mach number the test-section density is continuously controllable. For one run the M = 1.3 nozzle was operated subsonically to check the compatability of the two tunnels at about the same Mach number.

Description of Models

The two configurations tested simulated the upper and lower vertical tails of an air-to-ground missile. These two configurations were similar in several respects. For example, both surfaces had their leading edges swept back 60° and both surfaces were equipped with unbalanced rudders hinged at the leading edge of the rudder. The two configurations differed

primarily in the root fixity and in plan-form details at the tip. The upper vertical tail plan form was 1/10 scale and had an aspect ratio of 0.63 and a taper ratio of 0.34. The lower vertical tail was 1/7 scale and had an aspect ratio of 0.72 and a taper ratio of 0.43. Models of both configurations had flat-plate airfoil sections with beveled leading and trailing edges. The models were cut from 2024-T aluminum-sheet stock and tapered in thickness by a chemical milling process. The plan-form dimensions of the two configurations and the design thickness distribution of all the models tested are shown in figure 1. Models of different thicknesses indicated by the numerical designations were used in order to obtain flutter points within the limitations of the two tunnels. The actual measured thicknesses of the lower surface models were about 15 percent thicker than the design thickness and the upper surface models varied from the design thickness by about ±0.003 inch.

The models were mounted on the tunnel wall with two different types of simulated fuselage mounts as shown in figure 2. In figure 2(b) the upper portion of the clamp has been removed to show the method of clamping. The mount used in the supersonic tests placed the root chord about 3/4 inch away from the wall, whereas the mount used in the transonic tunnel placed the root chord about 3 inches away from the wall. The primary purpose of these simulated fuselages was to remove the models from the tunnel-wall boundary layer.

The lower surface models had an integral base block which provided clamping along the entire root chord. The upper surface models had a root fixture (see figs. 1(b) and 3) which simulated the fuselage attachment fittings of the prototype.

The rudders of the models were made by cutting the outline of the rudder from the model except for a small portion near the hinge line near the root. The outer portion of the rudder was held to the fin by means of nylon thread hinges. These hinges were made by drilling a small hole on each side at the hinge line, drawing a small nylon thread through the holes so as to form a figure eight, and then gluing the thread at the holes. The model rudder rotation frequencies were tuned to the desired values by varying the amount of retaining metal at the hinge line near the root. (See fig. 3(b).) In some cases for the lower surface it was necessary to lower the bending frequency by making small cuts parallel to the air flow at the root chord.

The models were equipped with an electrical-resistance-wire strain-gage bridge oriented to be sensitive to the flutter mode.

The masses and natural vibration frequencies of the various models tested are presented in table I. In the "Model Number" column, the letters A, B, C, D suffixed to the numerical designations indicated duplicate models for each thickness series. The first four natural
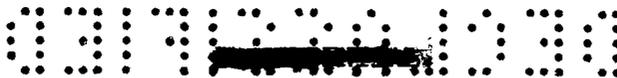
vibration modes measured for models 11-B and 25-B are presented in figures 4 and 5. These measured modes are considered to be representative of all the models tested. These modes were obtained by the method used in reference 1. The modes are shown as three-dimensional drawings of the deflected models along with a table of deflections (normalized on the maximum deflection) at various points. The locations of these points are presented in figure 6 for both the upper and lower surfaces. The node lines for the lower surface are shown in figure 7(a) and those for the upper surface in figure 7(b).

Test Procedure

The test procedures used in the two wind tunnels were similar in that the Mach number was first established at the desired value and then the test section density was increased until flutter was observed. The tests in the two tunnels differed in that the time required to reach the flutter condition was only a few seconds in the supersonic flutter tunnel whereas the time required in the transonic tunnel was several minutes. As will be noted subsequently, the agreement indicated by the data from the two facilities implies that these and other differences between the two tests had insignificant effects on the results.

For the tests in the supersonic tunnel the model strain-gage output as well as tunnel conditions were recorded for the entire run by utilizing an oscillograph. In the transonic tunnel the strain-gage output from the model was recorded continuously by using a magnetic tape recorder equipped with a frequency modulation system. In this manner, a record of the flutter condition could be obtained even though the model might be destroyed in too short a period of time for a record to have been obtained otherwise.

RESULTS AND DISCUSSION

The basic data obtained in this investigation are presented in table I and figures 8 and 9. Figure 8 shows the variation of the altitude-stiffness parameter $\frac{b\omega_\beta}{a}\sqrt{\mu}$ with Mach number. The altitude-stiffness parameter values shown are based on the semichord b at the three-quarter-span station. For the lower surface the value of b used was 0.203 foot, whereas for the upper surface b was 0.214 foot. The frequency ω_β used in calculating values of the parameter is the measured frequency of the second mode for all the models. This second mode resembles a rudder rotation mode and will be referred to as such subsequently. For the lower surface the mass-ratio parameter μ is defined as the ratio of the mass of the exposed model to the mass of the volume of air contained in the conical frustrum whose height is the model span and whose bases have

diameters equal to the root chord and the tip chord. For the upper surface, which has a rounded tip, the mass ratio is defined in the same manner except that an extrapolated tip chord which is obtained by extending the trailing edge to the tip is used. For the lower surface the volume was 0.0743 cubic foot whereas for the upper control it was 0.0874 cubic foot.

Figure 8(a) indicates that the altitude-stiffness parameter for the upper surface had a conventional variation with Mach number, that is, it increased almost linearly to a high value near $M = 1.0$ and then, after a small decrease, increased to higher values near $M = 3.0$. This type of flutter boundary has been observed for a variety of configurations.

In figure 8(b) the flutter boundary for the lower surface exhibits somewhat unusual behavior. The flutter boundary is composed of two segments which resemble conventional flutter behavior except that the two segments are separated by a discrete jump at a Mach number of about 1.18. This jump in the parameter corresponds to a decrease of about 50 percent in the density required to produce flutter. This decrease is associated with a change in the mode of flutter as evidenced by the change in flutter frequency shown in figure 9. Figure 9(b) indicates that the flutter frequency for the lower surface increased discontinuously from a frequency slightly below the rudder rotation frequency to values somewhat higher than the rudder rotation frequency. This change in mode occurred at the same Mach number as that at which the decrease in flutter density occurred. A sudden change of flutter mode with associated changes in the flutter boundary has been observed before for other configurations. (See ref. 2.)

Figure 9(a) indicates that the flutter mode for the upper fin underwent similar changes through the Mach number range except that the change from a low frequency mode to a higher frequency mode required a much larger change in Mach number.

The possibility of a reflected shock wave causing the abrupt change in flutter mode has been considered. Construction of a Mach angle diagram for the lower surface model at $M = 1.3$ in the supersonic tunnel indicates that the shock reflected from the tunnel side wall would intercept the model tip. However, a similar estimate of reflected-shock conditions in the larger transonic tunnel indicates that the reflected shock should clear the model at Mach numbers greater than $M = 1.05$. The relatively smooth variation of the data through this Mach number would indicate little effect of reflected shocks on the data. Furthermore, it might be noted that the generally good agreement indicated by the data from the two testing facilities lends credence to the data as a whole.

Some speculative remarks may be in order concerning a possible cause for the observed change in mode. It is noted in figure 1 that the trailing edge of the lower surface model is at an angle of $58.4°$ with the airstream
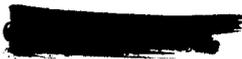
direction. The Mach number which has a Mach angle corresponding to this trailing-edge angle is about 1.17 - in other words, very near the Mach number at which the change in flutter mode occurred. When the Mach angle reaches the trailing-edge angle, certain changes in the flow conditions can be expected. For example, disturbances originating at the trailing-edge root intersection can no longer be propagated onto the surface. The possible importance of this observation can be judged by examination of the rudder-rotation deflection mode shown in figure 4(b) which indicates that the largest deflections in this mode occur at the intersection of the trailing edge and the root. Another change in flow conditions which occurs at this Mach number is that the shed vorticity in the wake can no longer induce forces on the surface.

Further substantiation of these remarks is offered by the data of reference 2 which indicate a change in flutter mode for delta configurations at M = 1.0. The data obtained for the upper surface in this investigation do not contradict the foregoing statements in that the gradual change in flutter mode which occurred for this configuration can be said to have occurred near M = 1.29, the Mach number having a Mach angle equal to the trailing-edge angle.

CONCLUDING REMARKS

Flutter models of the upper and lower vertical tails of an air-to-ground missile have been tested in the Mach number range from 0.5 to 3.0. It was found that the upper surface exhibited more or less conventional flutter behavior throughout the Mach number range whereas the lower surface experienced a sudden change in flutter mode at a Mach number of about 1.18. This change in flutter mode was accompanied by a decrease of about 50 percent in the density required for flutter to occur.

Langley Aeronautical Laboratory,
    National Advisory Committee for Aeronautics,
        Langley Field, Va., March 28, 1957.
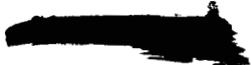
REFERENCES

1. Hanson, Perry W., and Tuovila, W. J.: Experimentally Determined Natural Vibration Modes of Some Cantilever-Wing Flutter Models by Using an Acceleration Method. NACA TN 4010, 1957.

2. Jones, George W., Jr., and Young, Lou S., Jr.: Transonic Flutter Investigation of Two 64° Delta Wings With Simulated Streamwise Rib and Orthogonal Spar Construction. NACA RM L56I27, 1957.
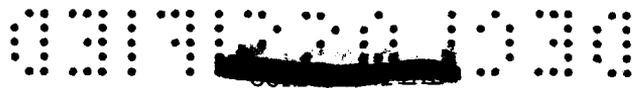
TABLE I.- BASIC DATA

(a) Lower vertical tail

Run	Model	Frequency, cps				ω_f/ω_β	Mass of model, slugs	ρ	a	M	$b\omega_\beta/a$	μ	$\dfrac{b\omega_\beta}{a}\sqrt{\mu}$
		1st mode	2d mode	3d mode	Flutter mode								
T-1	9-B	41.3	119.0	145.4	-----	-----	0.00327	0.002099	494	0.984	0.307	21.0	1.41
T-2	17-B	41.6	108.7	135.7	93.5	0.860	.00312	.001660	493	1.055	.281	25.3	1.41
T-3	17-B	41.7	108.8	135.3	94.4	.868	.00312	.001562	512	1.151	.271	26.9	1.41
T-4	17-C	41.7	110.7	130.0	86.4	.781	.00312	.002108	501	.846	.282	19.9	1.26
T-5	15-B	23.5	60.7	72.9	47.8	.787	.00176	.000077	1063	.874	.0728	307.6	1.28
T-6	7-D	34.6	90.4	111.0	104.8	1.16	.00231	.000386	530	1.236	.218	80.5	1.96
T-7	7-D	*34.6	*90.4	111.0	81.4	.900	.00231	.003151	508	.510	.227	9.87	.713
T-8	7-D	*34.6	*90.4	111.0	105.0	1.162	.00231	.000485	504	1.202	.229	64.1	1.83
T-10	9-C	-----	115.0	-----	95.2	.828	.00327	.002196	494	.974	.297	20.0	1.33
S-10	13-B	65	156	201	188.0	1.205	.00472	.000706	990	1.3	.201	89.7	1.905
S-11	13-B	*65	*156	201	186	1.192	.00472	.00079	995	1.3	.200	80.3	1.79
S-13	11-B	57	148	173	152	1.027	.00394	.000826	931	1.64	.203	64.2	1.625
S-14	13-C	67	175	209	188	1.074	.00464	.00128	873	2.0	.256	49.5	1.80
S-16	11-D	58	148	185	169	1.142	.00394	.000891	731	3.0	.258	62.4	2.04
S-17	13-D	66	170	207	194	1.141	.00472	.000645	991	1.3	.219	98.3	2.16
S-18	11-C	57	143	183	116	.812	.00394	.00218	1105	.58	.165	24.9	.822

*Assumed to be the same value.

DECLASSIFIED

TABLE I.- BASIC DATA - Concluded.

(b) Upper vertical tail

Run	Model	Frequency, cps				Flutter mode	ω_f/ω_β	Mass of model, slugs	ρ	a	M	$b\omega_\beta/a$	μ	$\dfrac{b\omega_\beta}{a}\sqrt{\mu}$
		1st mode	2d mode	3d mode	4th mode									
TU-1	21-B	26.5	87.1	132.3	255.0	-----	-----	0.00424	0.001821	544	0.833	0.215	26.6	1.11
TU-2	21-A	26.9	88.8	131.5	260.5	-----	-----	.00407	.001599	497	1.023	.240	29.1	1.30
TU-3	21-C	27.6	88.9	128.5	253.8	-----	-----	.00388	.001264	483	1.120	.246	35.1	1.46
TU-4	21-D	25.8	86.2	124.0	269.3	72.2	0.838	.00393	.001240	498	1.184	.233	36.3	1.44
TU-5	27-C	25.8	83.8	124.5	238.1	51.4	.614	.00383	.000958	534	.991	.211	45.7	1.42
TU-6-1	19-A	22.0	71.0	104.5	201.0	63.2	.890	.00311	.002510	499	.512	.191	16.0	.764
TU-6-2	19-A	*22.0	*71.0	*104.5	*201.0	63.0	.887	.00311	.002778	498	.494	.192	12.8	.687
TU-7	27-A	24.3	82.4	118.0	226.2	52.6	.638	.00367	.001006	488	1.079	.227	41.7	1.47
TU-8-1	27-A	24.1	83.3	118.0	225.3	55.0	.668	.00367	.001293	486	.926	.228	32.5	1.30
TU-8-2	27-A	*24.1	*83.3	*118.0	*225.3	51.6	.627	.00367	.001085	484	.960	.229	38.7	1.42
TU-8-3	27-A	*24.1	*83.3	*118.0	*225.3	56.9	.692	.00367	.001367	486	.898	.228	30.7	1.26
TU-9-1	27-B	24.7	83.4	118.3	263.6	58.3	.699	.00371	.001209	490	1.013	.229	35.1	1.36
SU-1	25-D	34	117	170	325	110	.940	.00533	.000872	986	1.3	.160	70	1.335
SU-2	25-B	34.4	111.2	170.5	329	125	1.125	.00533	.000913	924	1.64	.162	66.8	1.324
SU-3	25-A	34.6	121.8	172.2	344	140	1.150	.00518	.001000	848	2.0	.193	59.3	1.488
SU-5	23-D	33.3	112.7	160	315	125	1.110	.00502	.000723	722	3.0	.210	79.5	1.872
SU-7	23-B	33.4	113.4	162	312	104	.918	.00495	.000743	986	1.3	.155	76.3	1.353

*Assumed to be the same value.

(b) Upper vertical tail.

Model number	t_R	t_T	t_{B_1}	t_{B_2}
19	.044	.021	.085	.211
21	.059	.028	.115	.285
23	.073	.035	.142	.354
25	.082	.039	.159	.395
27	.053	.025	.102	.255

(a) Lower vertical tail.
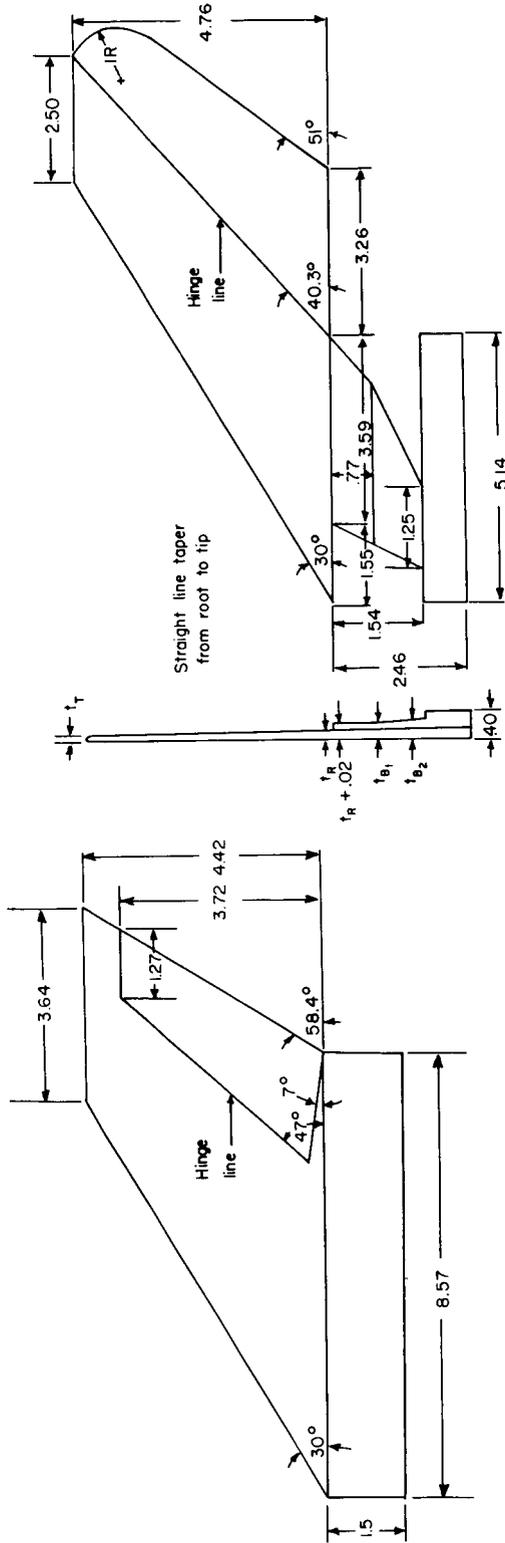
Model number	t_R	t_T
7	.035	.015
9	.048	.020
11	.059	.025
13	.066	.028
15	.026	.011
17	.042	.018

Figure 1.- Line drawing of models with pertinent dimensions in inches.

DECLASSIFIED

(a) Langley 2- by 2-foot transonic flutter tunnel.
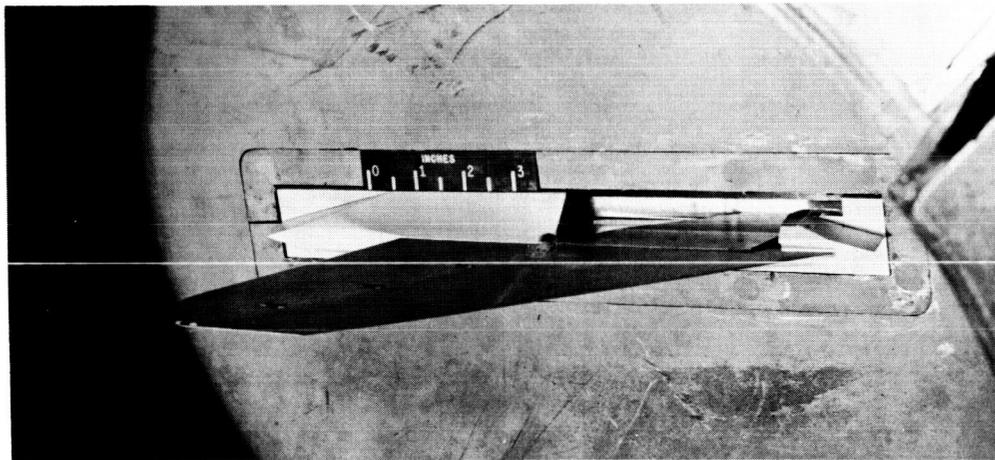
L-57-1553

(b) Langley 9- by 18-inch supersonic flutter tunnel.

Figure 2.- Photographs of models mounted in wind tunnels.
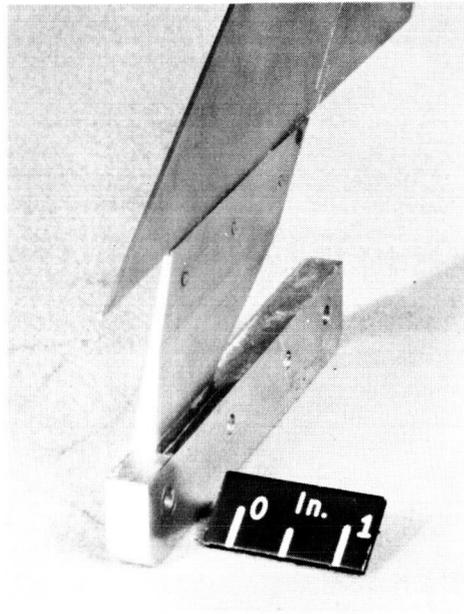
(a) Detail of attachment fitting.
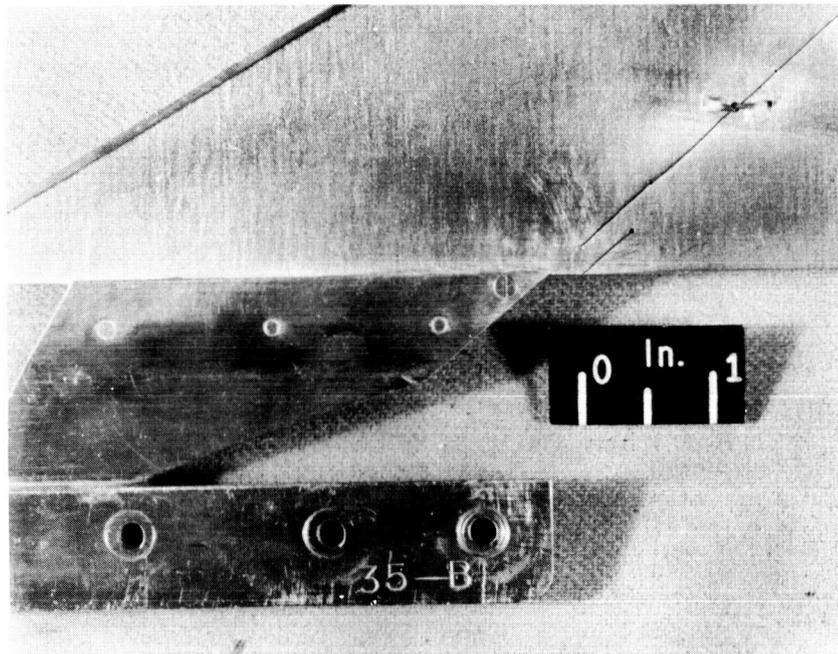
(b) Detail of method of hinging rudder.   L-57-1554

Figure 3.- Photographs of root area of upper surface model.
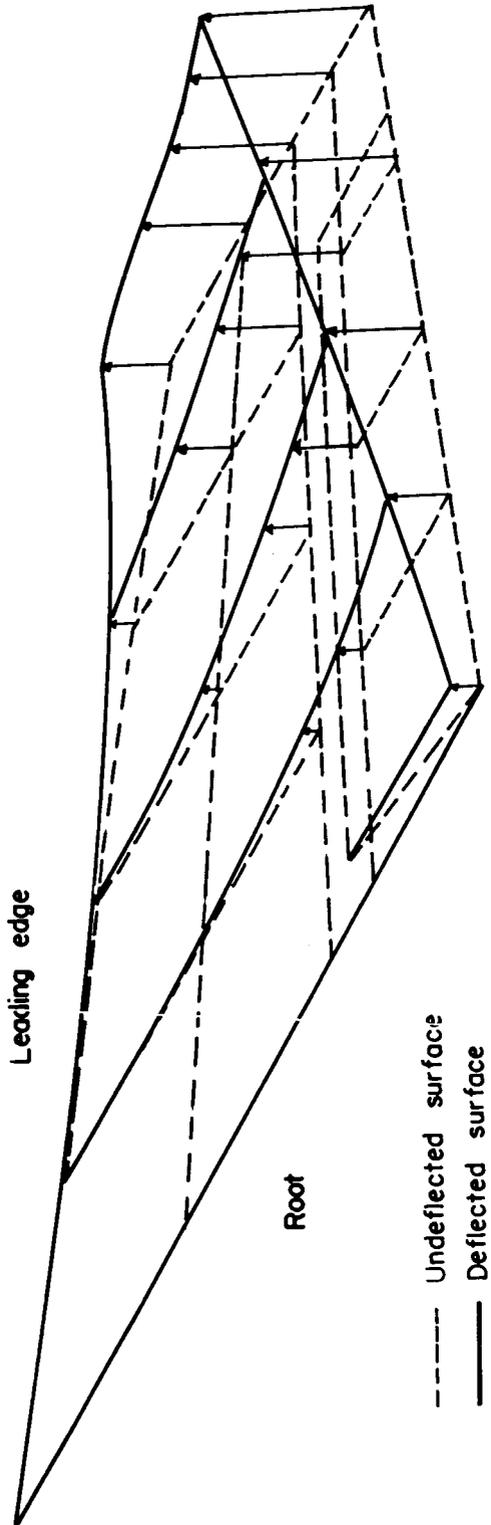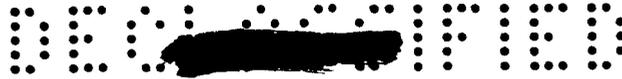
Leading edge

Root

– – – – Undeflected surface
———— Deflected surface

Point	Deflection	Point	Deflection	Point	Deflection	Point	Deflection	Point	Deflection
A_1	0	B_1	0	C_1	0	D_1	.05	E_1	.17
A_2	.01	B_2	.03	C_2	.11	D_2	.17	E_2	.37
A_3	.04	B_3	.13	C_3	.28	D_3	.38	E_3	.57
A_4	.17	B_4	.36	C_4	.53	D_4	.63	E_4	.78
A_5	.41	B_5	.62	C_5	.76	D_5	.87	E_5	1.00

(a) First mode; 58 cps.

Figure 4.- Lower surface natural mode shapes.
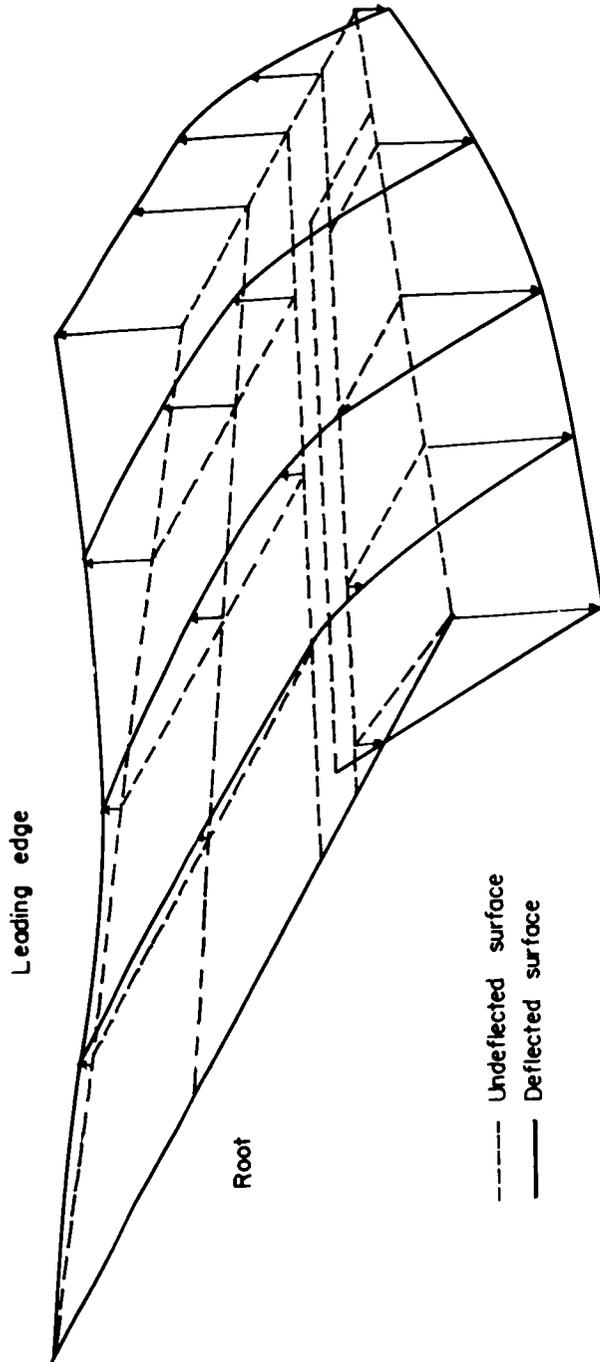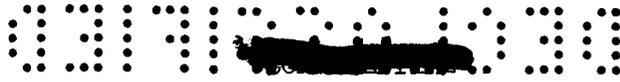
Leading edge

Root

----- Undeflected surface
——— Deflected surface

Point	Deflection	Point	Deflection	Point	Deflection	Point	Deflection	Point	Deflection
A_1	0	B_1	0	C_1	0	D_1	-.17	E_1	-1.00
A_2	.07	B_2	.05	C_2	.05	D_2	-.16	E_2	-1.00
A_3	.21	B_3	.21	C_3	.17	D_3	-.11	E_3	-.95
A_4	.48	B_4	.50	C_4	.43	D_4	.02	E_4	-.66
A_5	.86	B_5	.78	C_5	.75	D_5	.44	E_5	-.24

(b) Second mode; 155 cps.

Figure 4.- Continued.
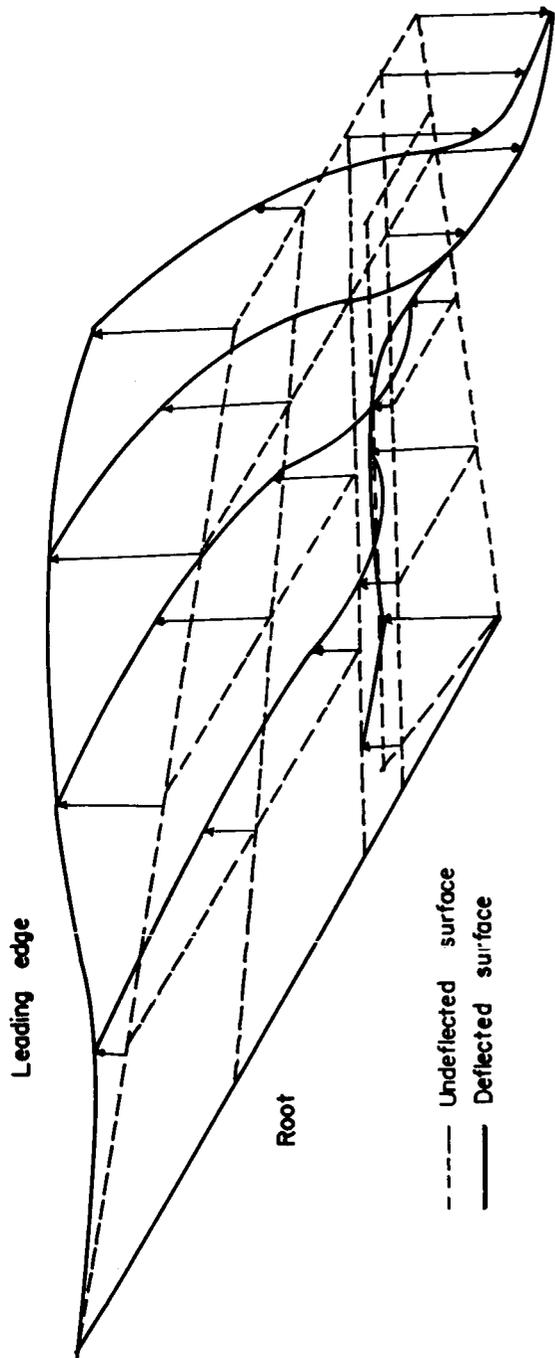
DECLASSIFIED

Leading edge

Root

- - - - Undeflected surface
───── Deflected surface

Point	Deflection	Point	Deflection	Point	Deflection	Point	Deflection	Point	Deflection
A_1	0	B_1	0	C_1	0	D_1	.27	E_1	.83
A_2	.16	B_2	.34	C_2	.30	D_2	.28	E_2	.72
A_3	.68	B_3	.75	C_3	.55	D_3	.14	E_3	.33
A_4	1.00	B_4	.85	C_4	.05	D_4	-.57	E_4	-.58
A_5	.96	B_5	.37	C_5	-.98	D_5	-.96	E_5	-.91

(c) Third mode; 176 cps.

Figure 4.- Continued.
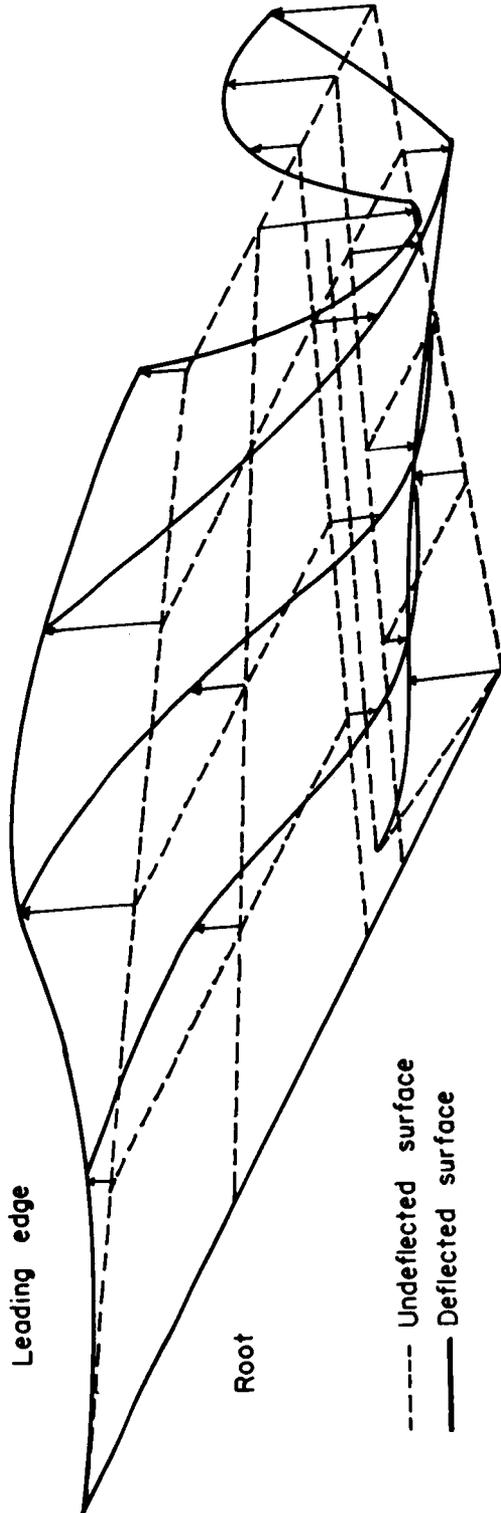
Leading edge

Root

----- Undeflected surface
——— Deflected surface

Point	Deflection	Point	Deflection	Point	Deflection	Point	Deflection	Point	Deflection
A_1	0	B_1	0	C_1	0	D_1	.05	E_1	.53
A_2	.15	B_2	.28	C_2	-.12	D_2	-.14	E_2	.33
A_3	.71	B_3	.35	C_3	-.29	D_3	-.31	E_3	.04
A_4	.75	B_4	-.03	C_4	-.40	D_4	-.37	E_4	-.31
A_5	.28	B_5	-1.00	C_5	.27	D_5	.71	E_5	.67

(d) Fourth mode; 328 cps.

Figure 4.- Concluded.
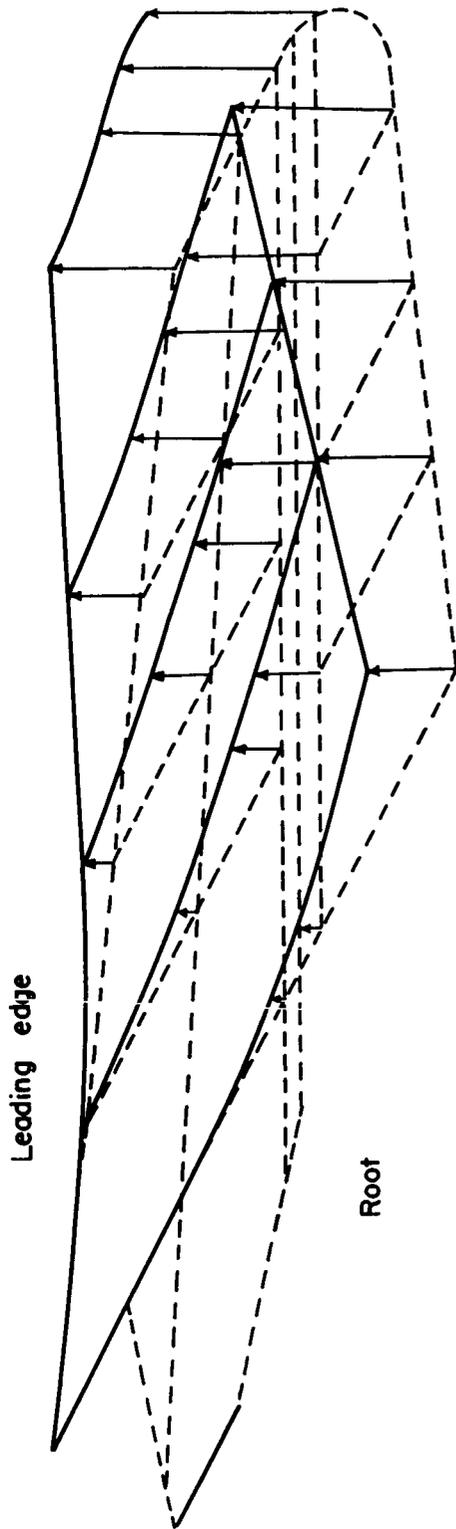
Leading edge

Root

--- Undeflected surface
— Deflected surface

Point	Deflection	Point	Deflection	Point	Deflection	Point	Deflection	Point	Deflection
A_1	.01	B_1	.02	C_1	.06	D_1	.14	E_1	.51
A_2	.02	B_2	.14	C_2	.30	D_2	.38	E_2	.68
A_3	.17	B_3	.34	C_3	.50	D_3	.57	E_3	.81
A_4	.43	B_4	.56	C_4	.68	D_4	.77	E_4	.94
A_5	.74	B_5	.81	C_5	.92	D_5	1.00		

(a) First mode; 34 cps.

Figure 5.- Upper surface natural mode shapes.
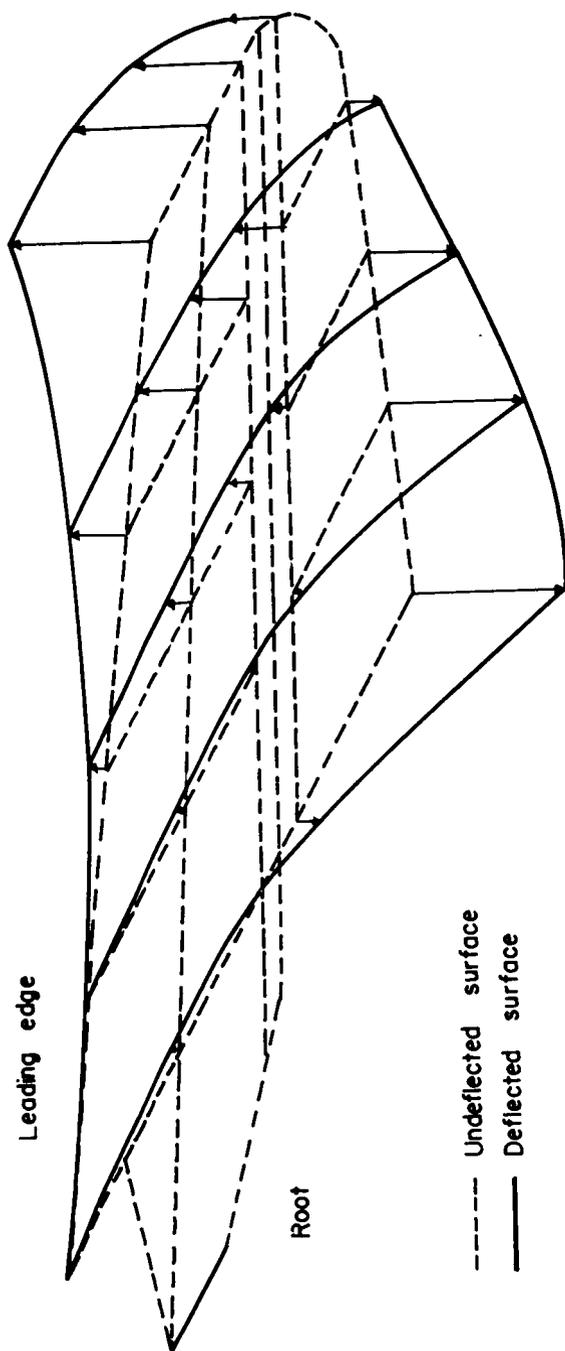
Leading edge

Root

– – – Undeflected surface
——— Deflected surface

Point	Deflection	Point	Deflection	Point	Deflection	Point	Deflection	Point	Deflection
A_1	.01	B_1	.01	C_1	.01	D_1	-.18	E_1	-1.00
A_2	.03	B_2	.03	C_2	.04	D_2	-.09	E_2	-.91
A_3	.13	B_3	.16	C_3	.16	D_3	.13	E_3	-.57
A_4	.36	B_4	.40	C_4	.36	D_4	.29	E_4	-.22
A_5	.92	B_5	.86	C_5	.72	D_5	.34		

(b) Second mode; 112 cps.

Figure 5.- Continued.
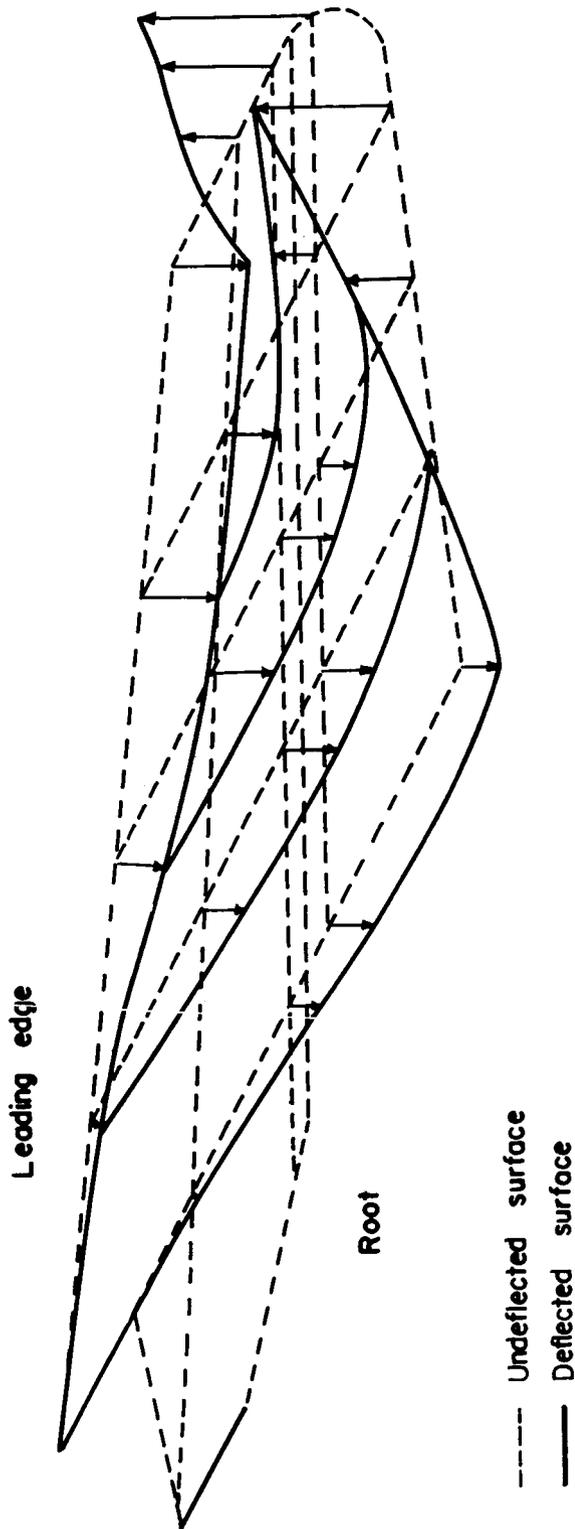
Leading edge

Root

--- Undeflected surface
— Deflected surface

Point	Deflection	Point	Deflection	Point	Deflection	Point	Deflection	Point	Deflection
A_1	0	B_1	-.05	C_1	-.19	D_1	-.24	E_1	-.23
A_2	-.07	B_2	-.26	C_2	-.31	D_2	-.29	E_2	.03
A_3	-.29	B_3	-.36	C_3	-.31	D_3	-.22	E_3	.37
A_4	-.44	B_4	-.30	C_4	0	D_4	.26	E_4	.78
A_5	-.44	B_5	.35	C_5	.64	D_5	1.00		

(c) Third mode; 169 cps.

Figure 5.- Continued.

Leading edge

Root

- - - Undeflected surface
— Deflected surface
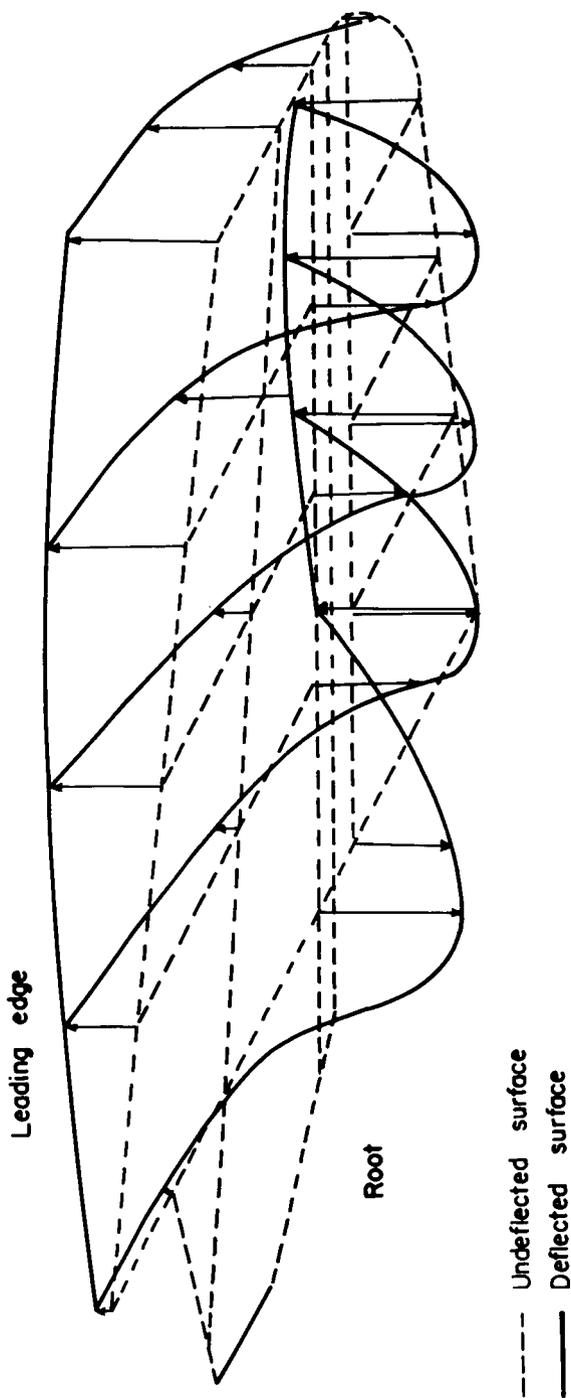
Point	Deflection	Point	Deflection	Point	Deflection	Point	Deflection	Point	Deflection
A_1	.10	B_1	-.05	C_1	-.89	D_1	-.54	E_1	1.00
A_2	.46	B_2	.14	C_2	-.71	D_2	-.78	E_2	.98
A_3	.71	B_3	.28	C_3	-.69	D_3	-.76	E_3	.94
A_4	.84	B_4	.56	C_4	-.71	D_4	-.79	E_4	.79
A_5	.97	B_5	.84	C_5	.57	D_5	-.15		

(d) Fourth mode; 320 cps.

Figure 5.- Concluded.

DECLASSIFIED
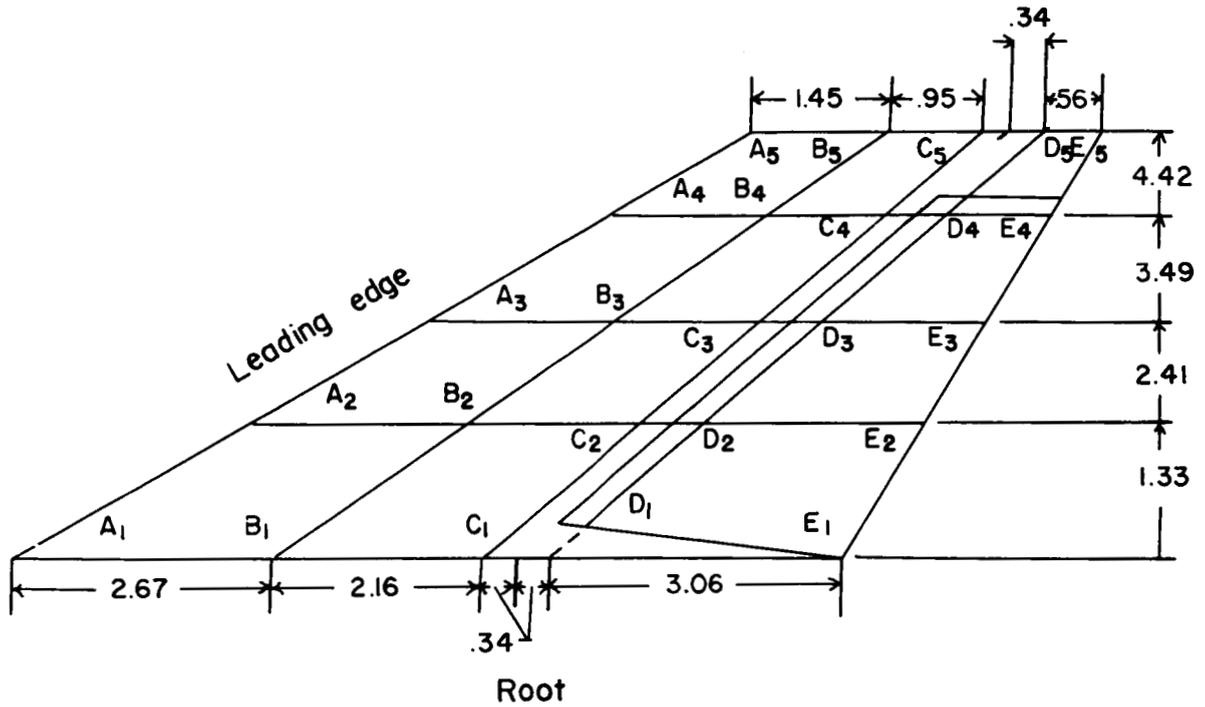
(a) Lower surface.

Figure 6.- Locations of deflection points. All dimensions are in inches.
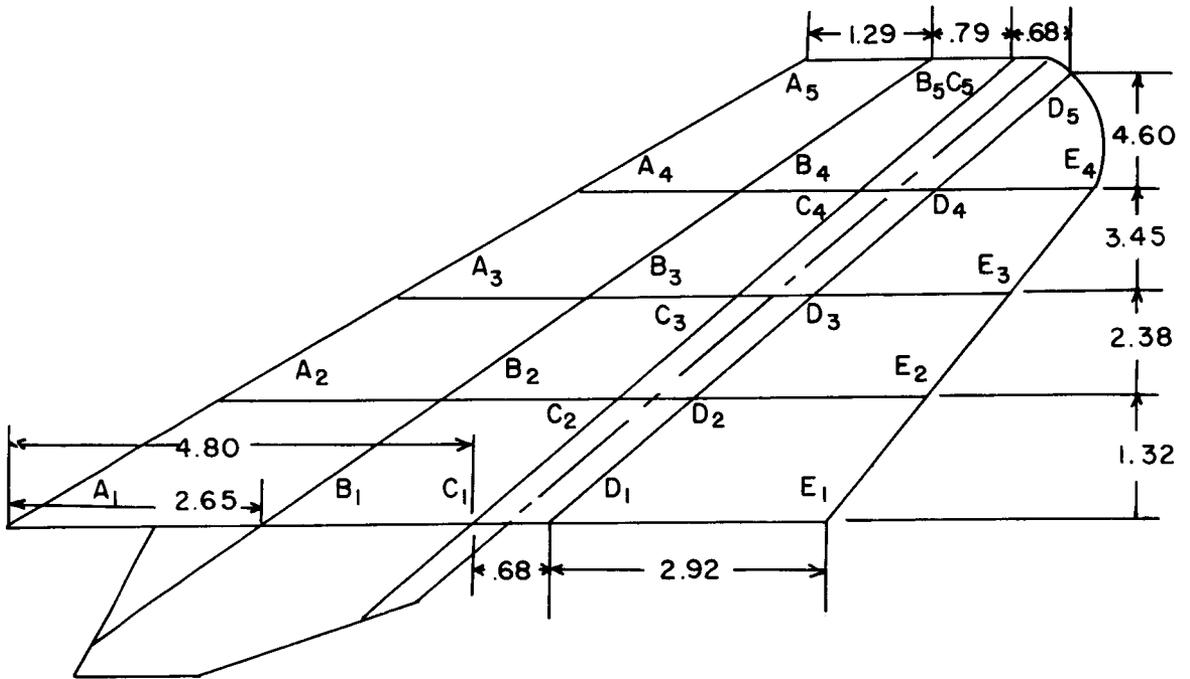
(b) Upper surface.

Figure 6.- Concluded.
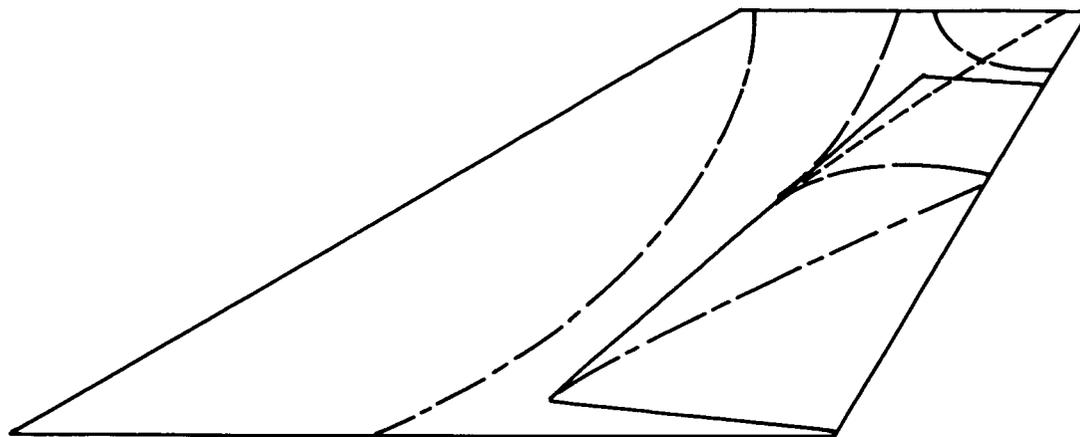
(a) Lower surface.
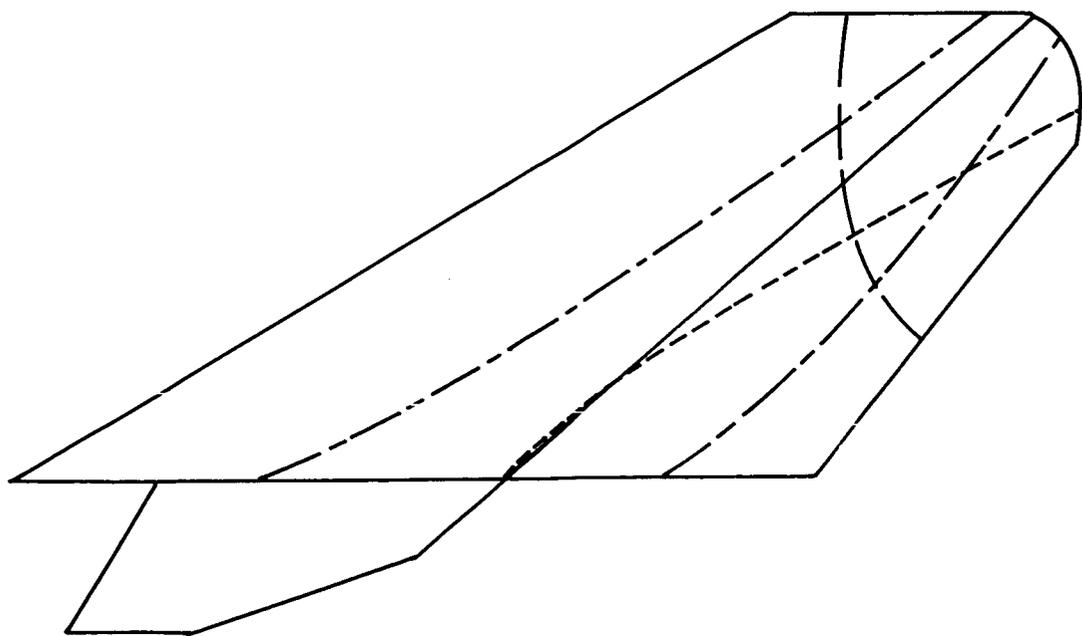
----- Second mode

— — Third mode

— - — Fourth mode

(b) Upper surface.

Figure 7.- Approximate positions of node lines.
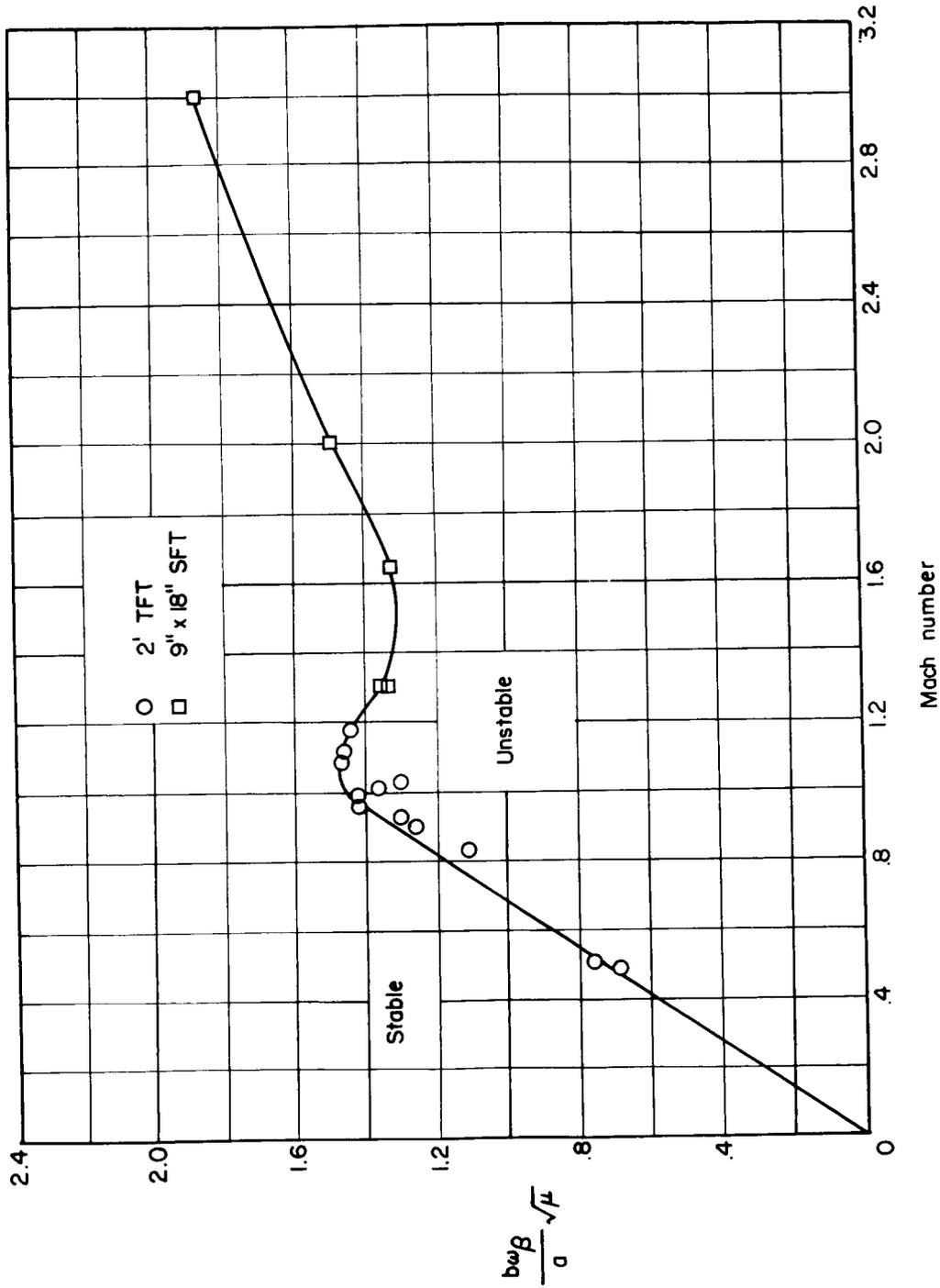
(a) Upper vertical tail.

Figure 8.- Variation of altitude-stiffness parameter with Mach number.
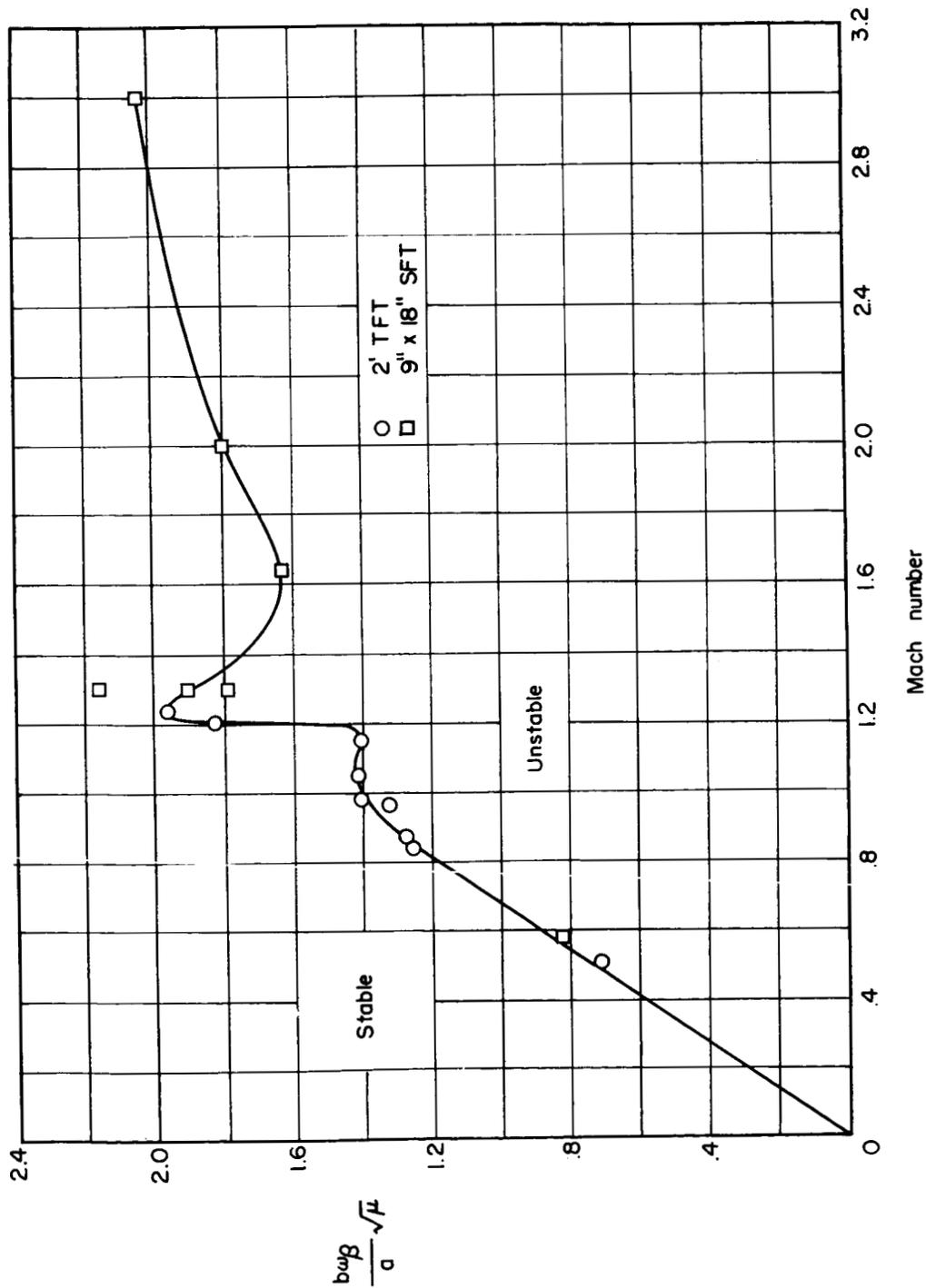
(b) Lower vertical tail.

Figure 8.- Concluded.
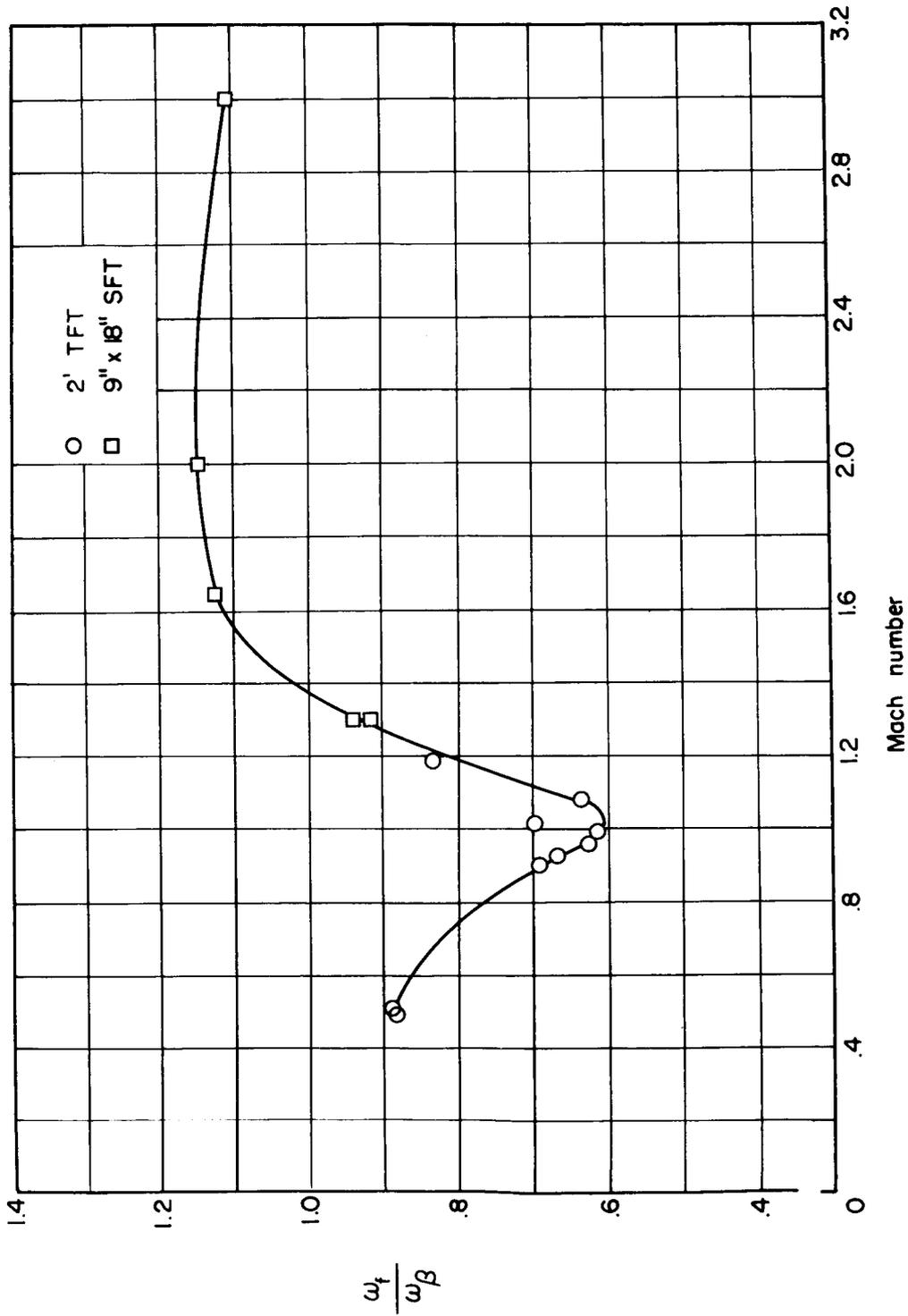
Figure 9.- Variation of ratio of flutter frequency to rudder rotation frequency with Mach number.

(a) Upper vertical tail.
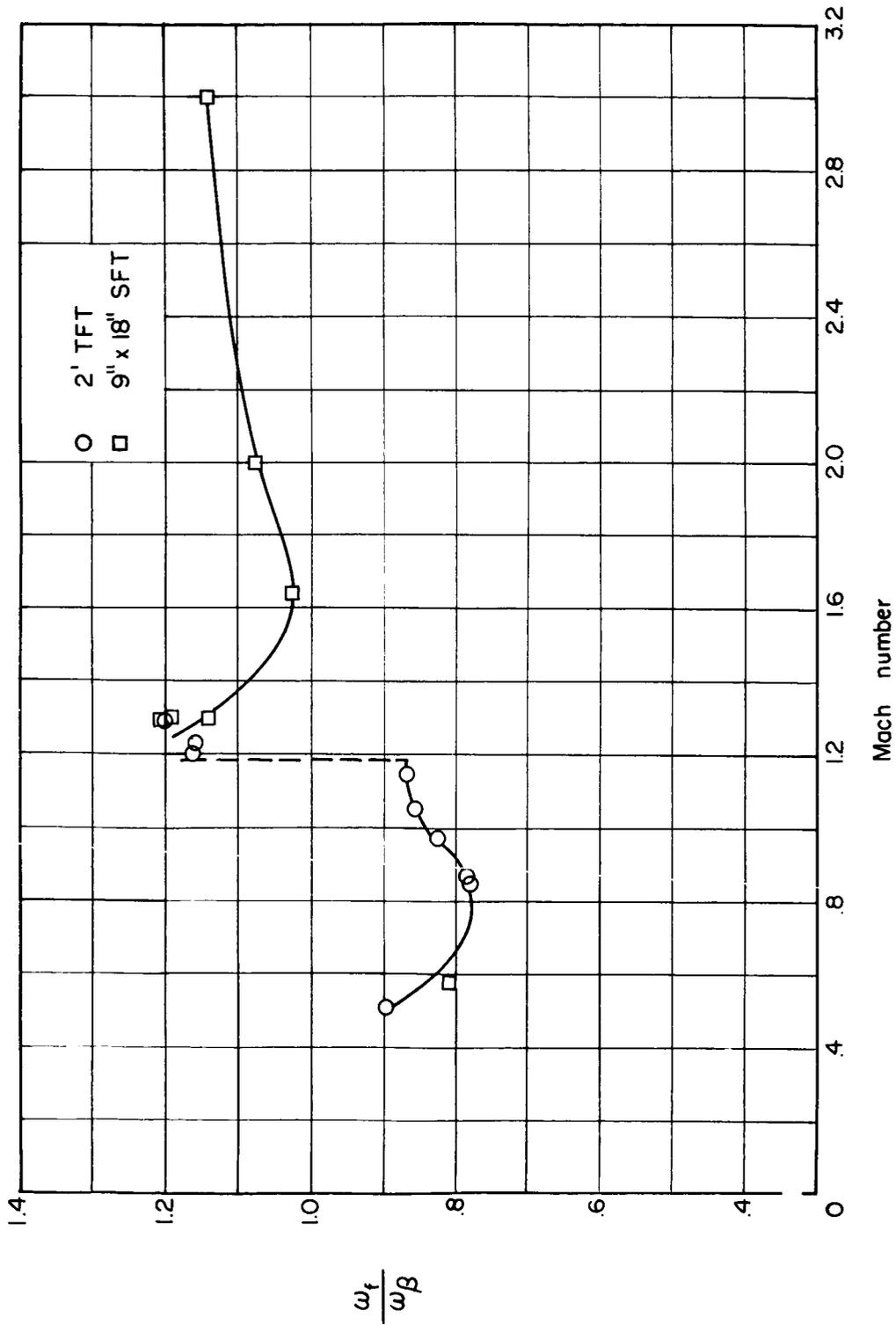
(b) Lower vertical tail.

Figure 9.- Concluded.